




# Adsorption, kinetics, and thermodynamic studies of cacao husk extracts in waterless sustainable dyeing of cotton fabric

Md. Yousuf Hossain · Wenju Zhu · Md. Nahid Pervez · Xiaojun Yang ·  
Shamima Sarker · Mohammad Mahbubul Hassan · Md. Ikram Ul Hoque ·  
Vincenzo Naddeo · Yingjie Cai 

Received: 26 October 2020 / Accepted: 24 December 2020

© The Author(s), under exclusive licence to Springer Nature B.V. part of Springer Nature 2021

**Abstract** Natural dyes exhibit a low dye uptake when cellulosic fiber dyeing is carried out using a conventional water bath dyeing process. In this research, cotton fabric was exhaust dyed in a microemulsion dyebath containing cacao husk extracts dye and decamethylcyclopentasiloxane (D5) to achieve higher dye exhaustion percentage on cotton fiber, which is an environmentally beneficial dyeing process. The adsorption behavior of cacao husk extract dye in a D5 microemulsion system was investigated under conditions of varied dye mass (1–8% o.w.f), dyeing time (5–500 min), and dyeing temperatures (333–373 K). Kinetic modelling of cacao husk extracts dye/D5 adsorption on cotton fiber was studied by fitting experimental data to pseudo first-order and pseudo second-order kinetics, and the intraparticle diffusion model. Early results indicated that the kinetic model of adsorption of cacao husk extracts dye on cotton fiber

followed the pseudo second-order model. Langmuir, Freundlich, and Dubinin–Radushkevich adsorption isotherm models were employed to analyze the adsorption isotherms, and the results showed that the adsorption process fit well with the Langmuir model compared to the Freundlich isotherm. The mean adsorption energy from the Dubinin–Radushkevich isotherm model implied that adsorption of the cacao husk extracts onto cotton was accompanied with a physical process. The values of standard enthalpy ( $\Delta H^\circ > 0$ ), standard entropy ( $\Delta S^\circ > 0$ ), and Gibbs free energy ( $\Delta G^\circ < 0$ ) strongly reflected that the adsorption of the cacao husk extracts onto cotton was thermodynamically favourable and feasible. Thus, waterless dyeing of cotton fabric using a natural dye/D5 system explores a sustainable dyeing technology with higher dye exhaustion percentage.

Md. Y. Hossain · W. Zhu · Md. N. Pervez ·  
X. Yang (✉) · Y. Cai (✉)  
Hubei Provincial Engineering Laboratory for Clean  
Production and High Value Utilization of Bio-based  
Textile Materials, Wuhan Textile University,  
Wuhan 430200, China  
e-mail: xjyang@wtu.edu.cn

Y. Cai  
e-mail: yingjiecai@wtu.edu.cn

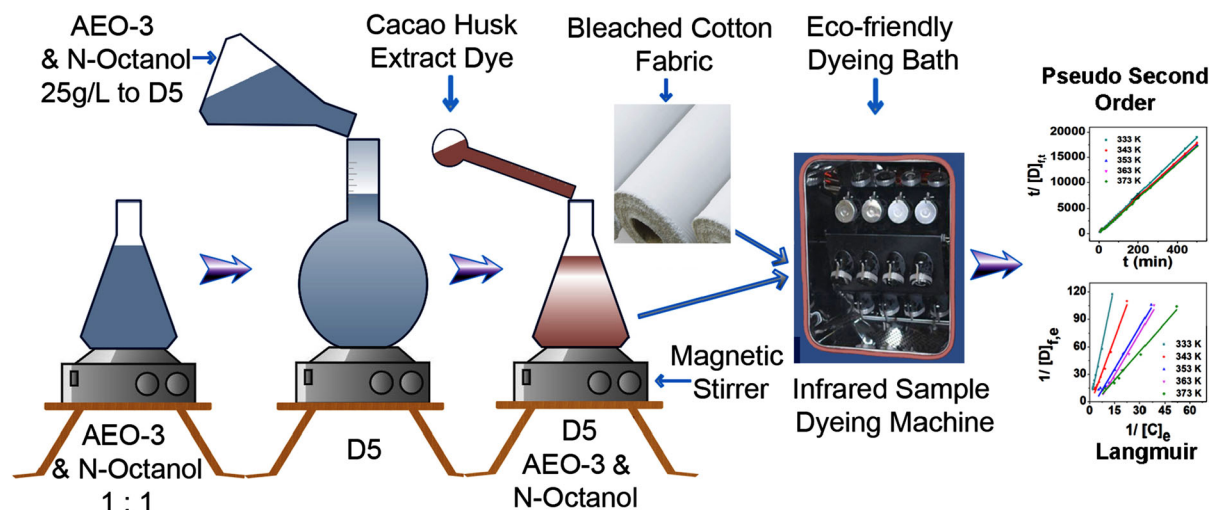
Md. Y. Hossain · X. Yang · Y. Cai  
Engineering Research Centre for Clean Production of  
Textile Dyeing and Printing, Ministry of Education,  
Wuhan Textile University, Wuhan 430200, China

Md. N. Pervez · V. Naddeo  
Sanitary Environmental Engineering Division (SEED),  
Department of Civil Engineering, University of Salerno,  
via Giovanni Paolo II 132, 84084 Fisciano,  
SA, Italy

S. Sarker  
College of Material Science and Engineering, Donghua  
University, Shanghai 201620, China

M. M. Hassan  
Bioproduct and Fiber Technology Team, AgResearch  
Limited, Lincoln 7647, New Zealand

## Graphic abstract



**Keywords** Cacao husk extracts · Natural dye · Decamethylcyclopentasiloxane · Adsorption · Thermodynamics

## Introduction

Synthetic dyes have been widely used for the dyeing of textile fibers due to their useful properties, such as reproducibility, abundance, wide ranges of color, convenience, and easy application process (Cai et al. 2018, 2020). However, most synthetic dyes used in the dyeing of textile fibers are not biodegradable, and some of them produce toxic degradation products. Moreover, traditional textile dyeing processes consume a substantial amount of water, energy, and auxiliaries and also produce a large volume of hazardous effluent, which are detrimental to the ecosystem and human health (Islam et al. 2018, 2019; Morshed et al. 2020; Pervez et al.

2020a, b). Therefore, a sustainable environmentally friendly textile dyeing process is highly attractive.

Consequently, there is a growing interest in utilizing natural dyes in textile fibers dyeing as they possess several good characteristics such as biodegradability, renewability, environmental compatibility, and other properties, such as anti-allergic, antibacterial, and UV protective functionalities (Gorjanc et al. 2016; Hong et al. 2012; Rehman et al. 2018). However, natural dyes exhibit low dye uptake and poor colorfastness to washing and rubbing while dyeing with cellulosic fibers, such as cotton (Samanta and Konar 2011). Though pretreatment can slightly improve the dye uptake rate and colorfastness, this process does not satisfactorily increase the dye uptake level (Tsatsaroni and Liakopoulou-Kyriakides 1995). Besides these, in the traditional natural dyeing process, the usage of heavy metal salts as mordants is not only harmful to the environment but also a challenging way to control color stability; therefore, the process is not suitable for large-scale production and application (Amutha and Sudhapiya 2020; İşmal and Yıldırım 2019). To solve the technical issues of low dye uptake rate of natural dyes on cotton fiber, it is necessary to ensure that a large amount of dye is adsorbed by the fiber from the dyebath. The uptake of natural dyes can be enhanced if they could be pigmented on cotton fiber.

Cacao is the fruit of the cacao tree (*Theobroma cacao*), a small evergreen tree of the Malvaceae family, and its seeds are cacao beans that are used to

Md. Ikram UlHoque  
Discipline of Chemistry, The University of Newcastle,  
University Drive, Callaghan, NSW 2308, Australia

Md. Ikram UlHoque  
Australian Institute for Bioengineering and  
Nanotechnology (AIBN), The University of Queensland,  
Brisbane, QLD 4072, Australia

make cacao butter and chocolate (Risner 2008). Cacao extracts are natural polyphenols prepared from the cacao husk. Cacao husk extracts dye (water-soluble) can produce brown shades in dyed textile cotton fibers (Hossain et al. 2020). It can be used as an effective and sustainable natural dye for the coloration of textile fibers as a non-toxic and eco-friendly dye for the dyeing of cellulosic fibers.

Non-aqueous dyeing is an ecologically responsive and green dyeing technology which has been employed as an alternative to the traditional water-based textile dyeing process (Chen et al. 2015; Pei et al. 2019). Water-soluble dyes have strong adsorption capacity in non-aqueous media (Tang and Kan 2020), but it is tough to dissolve water-soluble dyes in a non-aqueous medium (Pei et al. 2019). One dominant characteristic of the non-aqueous dyeing process is that a small amount of water is needed to dissolve the dye (Pei et al. 2019; Wang et al. 2018a). This dyeing system uses an organic solvent that helps to disperse the dye and facilitate the dyeing process. D5 has been employed as an organic solvent in the non-aqueous dyeing system. D5 solvent is a clear, colorless, non-toxic and odorless siloxane fluid, which is safe for humans and the environment (Pei et al. 2019; Tang et al. 2017), and D5 in the residual dyebath can be subsequently recycled and reused by a simple static separation system (Pei et al. 2019). Until now, a number of papers have focused on a D5 dyeing system with synthetic dyes, while very few researchers have reported on natural dyeing of textiles fibers using D5 solvent. Besides, the adsorption behavior of natural dyes in the non-aqueous dyeing system is still unclear and must be further investigated.

The cacao husk extracts were used as a natural dye in D5 medium for the dyeing of cotton fabric, and subsequently, the dyed cotton was treated by a fixation treatment with a cationic dye-fixing agent in the D5 medium (Hossain et al. 2020). The cotton fabric dyed with cacao husk extracts, exhibited better exhaustion in the D5 medium, higher fixation rate and color strength (K/S), and better colorfastness to washing and rubbing compared to the fabric dyed with the same extracts using the conventional aqueous dyeing and dye-fixing methods. The dye exhaustion percentage and dye fixation rate in the D5 medium were 95.6% and 94.8%, respectively, which are significantly higher when compared to conventional water medium dyeing with 48.2% dye exhaustion percentage and

35.3% dye fixation rate (Hossain et al. 2020). Due to its excellent dye exhaustion percentage in D5 medium, the exhaust waterless dyeing method was facilely applied for other soluble natural dyes. It is also worth understanding the adsorption kinetics, isotherms, and thermodynamics of the cacao husk extracts dye/D5 dyeing system.

The cacao husk extracts/D5 reverse micelle dyeing system comprised an organic solvent and miscible fluids stabilized by surfactants and co-surfactants. Surfactants and co-surfactants effectively reduced interfacial tension to form microemulsions (Salager et al. 2013). They created a ‘water pool’ where the water-soluble dyes were properly dispersed and formed an effective emulsion between the dye solution and D5 medium (Wang et al. 2016). When the dry and hydrophilic cotton fiber was immersed in the D5 dyebath, the ‘water pool’ evenly dispersed in the D5 medium, causing fast adsorption of the dye onto the fiber. After adsorption, the “water pool” was damaged. Besides, the adsorption processes were irreversible due to the hydrophobic property of D5. During the rotating dyeing process, the dye solution in D5 medium without dye aggregation (Wang et al. 2016) was continuously transferred from the D5 dye bath to the fiber, resulting in higher dye exhaustion compared to the conventional water medium dyeing. Of course, a small quantity of dye solution possibly desorbed if the “water pool” was not broken; meanwhile, the surfactants and co-surfactants adsorbed on the surface of the fiber also possibly contributed to impeding adsorption of the dye solution. Therefore, the dye solution was not completely absorbed into the fiber, i.e., 100% dye exhaustion (Fig. 1).

Therefore, the prime objective of this study is to execute the adsorption kinetics, isotherm, and

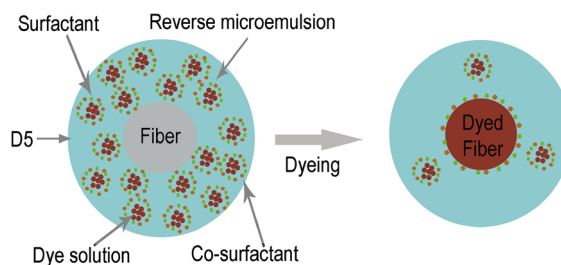


**Fig. 1** Schematic mechanism of cotton fiber dyeing in the cacao husk extracts/D5 microemulsion system

thermodynamic parameters of cacao husk extracts dye/D5 system to better understand the dyeing mechanism of natural dye in D5. The pseudo first-order and pseudo second-order models and intraparticle diffusion were plotted to clarify the kinetic behavior of cacao husk extracts dye. Further, the experimental data were fitted to Langmuir, Freundlich, and Dubinin–Radushkevich isotherm models to identify the adsorption mechanism. This study showed that the adsorption process of the dyeing followed the pseudo second-order kinetics and fit well with the Langmuir isotherm, and the adsorption of the cacao husk onto cotton was accompanied with a physical process.

## Experimental

### Materials

A pure desized, scoured, and bleached cotton woven fabric (GSM 140 g m<sup>-2</sup>, yarn count 40 s Ne) was received from Jiangnan Group Co., Ltd., China. Cacao husk extract natural dye (solid, water-soluble) was purchased from Organic Herb Inc., China, and used without further purification. Decamethylcyclopentasiloxane (D5 ≥ 95.0%) was obtained from Jiangxi Bluestar Xinghuo Silicones Co., Ltd., China, and utilized without additional purification. Alkylalcoholpolyoxyethylene ether (AEO-3) was purchased from Chengdu Aikeda Chemical Reagent Co., Ltd., China. N-octanol (≥ 99.0%) and ethanol (≥ 99.5%) were procured from Sinopharm Chemical Reagent Co., Ltd., China. All other chemicals and reagents were analytical grade.

### Dyeing of cotton in cacao husk extracts/D5 microemulsion dyebath

A predetermined amount of surfactant, AEO-3, and co-surfactant, n-octanol, were mixed at a mass ratio of 1:1 with mechanical stirring at room temperature to prepare a mixture (mixture 1). Subsequently, a fixed amount of mixture 1 was added to a D5 solution with continuous stirring at room temperature for preparation of homogeneous, stable, and transparent microemulsions (mixture 2) with 25 g L<sup>-1</sup> of the prepared mixture 1. Finally, a certain volume of cacao husk extracts dye solution containing 100% o.w.f (on the weight of fabric) of water (mixture 3) was slowly

added to mixture 2, and the resultant mixture was stirred until a stable and uniform cacao husk extracts dye/D5 microemulsion dyebath (mixture 4) was formed. Then, 2.0 g cotton fabric was immersed into the microemulsion dyebath (mixture 4) with a liquor-to-goods ratio of 20:1. The parameters of the dyeing process, such as dyeing temperatures (333–373 K), dyeing time (5–500 min), and cacao husk extract mass 1–8% o.w.f were varied. All dyeings were carried out in an infrared-heated laboratory dyeing machine (Model HB-HWX24, Ronggui Huibao Dyeing and Finishing Machinery Factory, China). A graphical illustration of the dyeing process of cotton fabric in the cacao husk extracts/D5 microemulsion dyebath is shown in Fig. 2a, and the dyeing profile is depicted in Fig. 2b.

### Dye exhaustion

Dye exhaustion means the amount of dye adsorbed by the fiber, and exhaustion percentage (E%) is determined by measuring the absorbance of cacao husk extract dyebath before and after dyeing, respectively. Ethanol was used to dilute the cacao husk natural dye/D5 microemulsion dyebath and allowed the dyes to uniformly disperse in the dyebath. A UV-Vis spectrophotometer (TU-1900 UV-VIS, PERSEE, China) was employed to measure the absorbance of the dyebath solution at the wavelength of maximum absorption (477 nm). The exhaustion percentage (E%) was calculated using Eq. 1 (Cai et al. 2018; Su et al. 2019).

$$E\% = \left( \frac{A_o - A_t}{A_o} \right) \times 100\% \quad (1)$$

where  $A_o$  is the absorbance of cacao husk extracts dye solution before dyeing and  $A_t$  is the absorbance of cacao husk extracts dye solution after dyeing.

### Dye adsorption in fiber

The amount of cacao husk extracts dye adsorbed  $[D]_{f,t}$  (g g<sup>-1</sup>) by per unit weight of the cotton fabric at time  $t$  (min) was calculated by using Eq. 1 (Haque et al. 2020).

$$[D]_{f,t} = \left( \frac{[C]_o - [C]_t}{m} \right) \times V \quad (2)$$

where  $C_o$  is the initial concentration ( $\text{g L}^{-1}$ ) of cacao husk extracts dyebath,  $C_t$  is the concentration ( $\text{g L}^{-1}$ ) of cacao husk extracts solution after time  $t$  (min),  $V$  is the volume of the cacao husk extracts dye solution (L), and  $m$  is the weight of cotton fabric (g) used for dyeing in the dyebath. After dyeing, the residual dyebath was diluted by ethanol, and its light absorbance value was measured by the UV-Vis spectrometer, subsequently the concentration of cacao husk extracts in the dyebath ( $C_t$ ) was calculated using a linear regression equation of the standard curve. Besides, the amount of cacao husk extracts dye adsorbed by per unit weight of the cotton fabric at equilibrium  $[D]_{f,e}$  ( $\text{g g}^{-1}$ ) was calculated using Eq. 2 (Haque et al. 2020).

$$[D]_{f,e} = \left( \frac{[C]_o - [C]_e}{m} \right) \times V \quad (3)$$

where  $C_e$  is the concentration of cacao husk extracts dye solution at equilibrium.

## Results and discussion

### Influence of dyeing time on the exhaustion percentage

The influence of dyeing time on the E% of cacao husk extract dye into the cotton fiber at different temperatures (333–373 K) with an applied dosage of 3% o.w.f of dye is shown in Fig. 3. It is worth noting that the cacao husk extracts dye was thermally stable at a higher dyeing temperature (Hossain et al. 2020), although some natural plant dyes are liable to thermal degradation above 343 K, for example, watermelon extracts (Liman et al. 2020). The thermal stability of cacao husk extracts dye proves that when dyeing of cotton fabric at high temperatures does not influence the detection of E% by using the absorbance. These results demonstrate that E% increased with increasing dyeing time, and the shortest equilibrium time was observed by 90 min at 363 and 373 K. Equilibrium times were found to be 100, 140, and 200 min at 353, 343, and 333 K, respectively. Higher temperatures led to shorter equilibrium time, and E% also increased with increasing temperature. At a higher temperature, E% was higher because the dye solution was more

quickly transferred from the microemulsion dyebath to the fiber. Once the dye solution was adsorbed on the fiber, it did not desorb and move back in the microemulsion dye bath since the adsorption was irreversible because of the hydrophilic properties of cellulosic fiber and hydrophobic properties of D5. The E% increased quickly in the initial stages and gradually decreased with increasing time until it reached equilibrium. It can be seen in Fig. 3 that the dyeing temperature had a significant influence on E% and the increased dyeing temperature leads to a rapid increase in dye exhaustion from 333 to 363 K. Interestingly, at 363 and 373 K, E% shows a similar tendency which implies that for cacao husk extract dyeing, 363 K is the optimal dyebath temperature to promote dye exhaustion into the fiber from the dyebath.

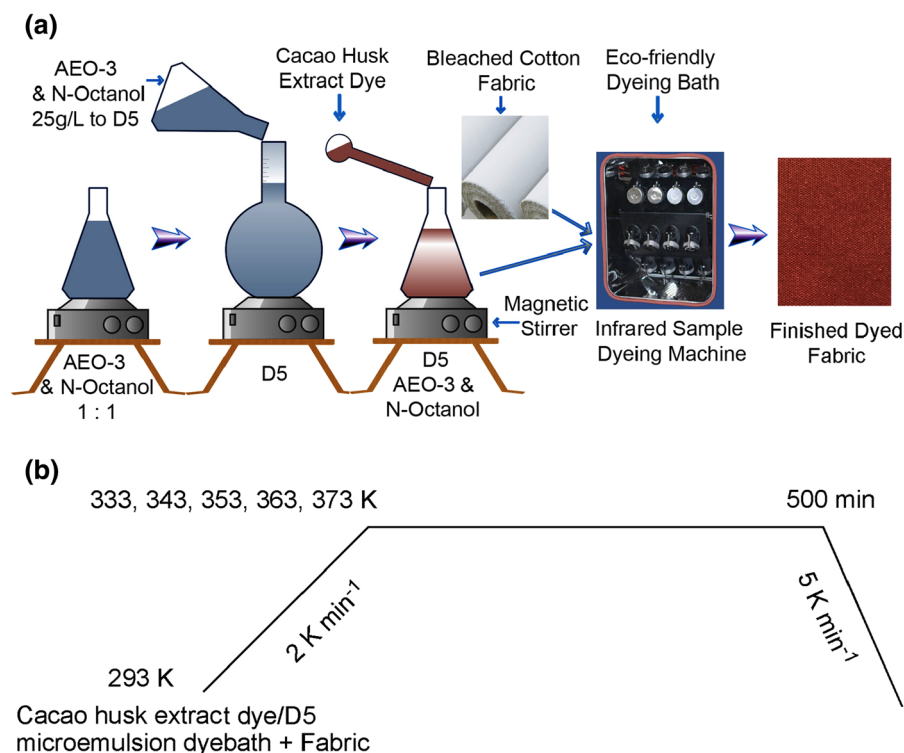
### Influence of cacao husk extract mass on exhaustion percentage

Figure 4 shows the E% versus cacao husk extracts dye mass at various dyeing temperatures (333–373 K). As shown in Fig. 4, E% increased with increasing cacao husk extracts mass until 3% o.w.f and then E% started decreasing with increasing dye mass above 3% o.w.f. However, with increased dye mass, the dye mass absorbed in the fiber still increased with mild promotion. Moreover, E% was also temperature-dependent, and maximum dye exhaustion was observed at a higher temperature. However, E% was found to be nearly similar at 353, 363, and 373 K.

### Influence of dyeing temperature on the exhaustion percentage

The influence of dyebath temperature on the E% of dyes was investigated in the range of 333–373 K temperatures and 3% o.w.f of cacao husk extract. This result (Fig. 5) indicates that the E% increased with increasing temperature and E% increased quickly from 333 to 363 K. When the temperature was at 373 K, the increasing rate of the exhaustion began to slow, which is similar to that at 363 K.





**Fig. 2** **a** Dyeing process and **b** dyeing profile of cotton fabric in the cacao husk extract dye/D5 microemulsion dyebath

Substantivity of cacao husk extract dye on cotton fabric

Substantivity plays a vital role in the dyeing process and is defined as the affinity between the substrate and dye molecules, and the substantivity is closely related to the affinity value defined by the thermodynamics of the dye (Ferus-Comelo 2013). Substantivity is generally applied to determine the suitability of a particular dye for a particular type of fiber. Substantivity represents the correlation among liquor-to-goods ratio, and the rate of exhaustion at equilibrium. Substantivity is calculated by using Eq. 3 (Cai et al. 2014).

$$K = \frac{E_e \times L}{100 - \%E_e} \quad (4)$$

where  $K$  is the substantivity;  $\%E_e$  is the percentage of dye exhaustion at equilibrium and  $L$  is the liquor-to-goods ratio. A higher  $K$  value suggests higher substantivity of cacao husk extracts dye toward cotton fiber and also higher transport of the dye from the dyebath to the fiber. A higher  $K$  value specifies that

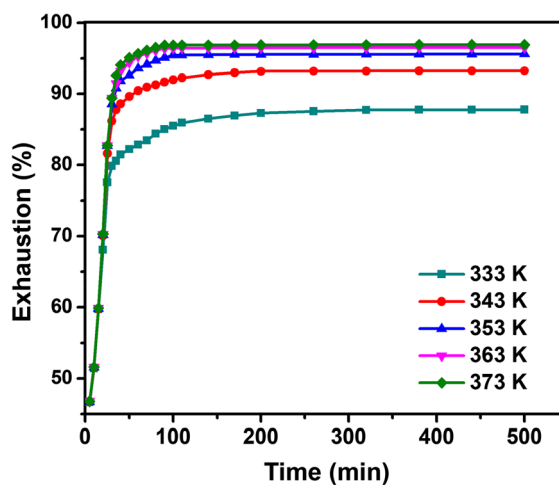


**Fig. 3** Influence of dyeing time (5–500 min) on  $E_e$  at different temperatures (333–373 K) with 3% o.w.f cacao husk extracts and a liquor ratio of 20:1

more dye could remain inside the fiber than the dyebath. The parameters of substantivity of dyeing are presented in Table 1. It can be seen from Table 1 that

the E% and substantivity (K) of cacao husk extract dye increased with increasing temperature in D5 microemulsion.

### Adsorption kinetics

The purpose of kinetic model analysis is to explain the dynamic adsorption interactions between cotton fiber and cacao husk extract dye. To evaluate the kinetics of cacao husk extract dye adsorption onto cotton fiber, experimental data were studied by using the Lagergren's pseudo first-order, pseudo second-order adsorption kinetic models, and intraparticle diffusion model (Moussout et al. 2018; Tang et al. 2019).

The pseudo first-order kinetic model can be expressed by Eq. 4 (Abraham et al. 2018; Khandaker et al. 2020).

$$\log([D]_{f,e} - [D]_{f,t}) = \log[D]_{f,e} - \left(\frac{K_1}{2.303}\right)t \quad (5)$$

where  $K_1$  ( $\text{min}^{-1}$ ) is the pseudo first-order adsorption rate constant. The correlation coefficient ( $R^2$ ), adsorption rate constant ( $K_1$ ), and equilibrium adsorption amount  $[D]_{f,e}$  (cal) are determined by employing the linear plot of  $\log([D]_{f,e} - [D]_{f,t})$  versus the adsorption time ( $t$ ). The fitted line plot is shown in Fig. 6a and the corresponding model fitting parameters of pseudo first-order are listed in Table 2. The correlation ( $R^2$ ) values determined from the pseudo first-order kinetic model are in the range of 0.9301–0.9677, indicating

that pseudo first-order model fit for adsorption of cacao husk extracts. Moreover, the  $[D]_{f,e}$  (cal) obtained from the calculation is less than the experimental  $[D]_{f,e}$  (exp) value demonstrating that the whole adsorption process cannot be described by the pseudo first-order model (Haque et al. 2020). The linear form of pseudo second-order adsorption kinetic model can be written as shown in Eq. 5 (Halysh et al. 2018; Simonin 2016).

$$\frac{t}{[D]_{f,t}} = \frac{1}{K_2[D]_{f,e}^2} + \left(\frac{1}{[D]_{f,e}}\right)t \quad (6)$$

where  $K_2$  ( $\text{g g}^{-1} \text{min}^{-1}$ ) is a pseudo second-order adsorption rate constant. Eq. 5 was employed to obtain the graph (Fig. 6b) from which  $[D]_{f,e}$  (cal),  $K_2$ , and  $R^2$  were determined and listed in Table 2. The pseudo second-order kinetic model describes the adsorption kinetics well with a higher correlation coefficient ( $R^2 = 0.99$ ). Furthermore, the pseudo second-order kinetic model exhibited closer values when comparing the experimental and calculated  $[D]_{f,e}$  values. The closer values between the calculated  $[D]_{f,e}$  (cal) and experimental  $[D]_{f,e}$  (exp) values suggest that the pseudo second-order model is well fitted to describe the adsorption kinetics of cacao husk extracts dye/D5 microemulsion dyeing of cotton fabric. With increasing dyeing temperature, the experimental  $[D]_{f,e}$  (exp) and calculated  $[D]_{f,e}$  (cal) values increased, reflecting higher temperatures led to

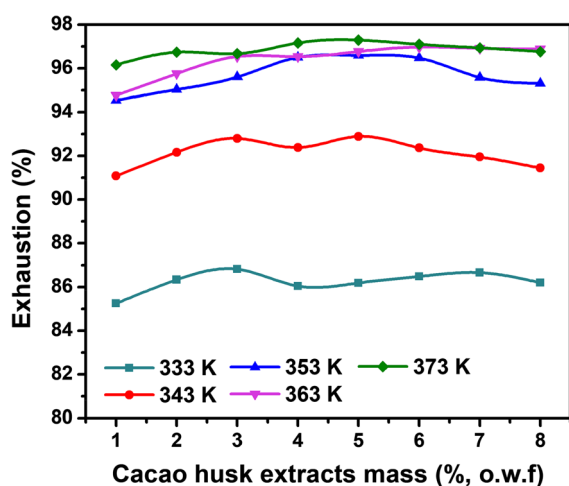


**Fig. 4** Influence of cacao husk extract mass (% o.w.f) on E% at different temperatures (333–373 K) for 90 min dyeing time with a liquor ratio of 20:1

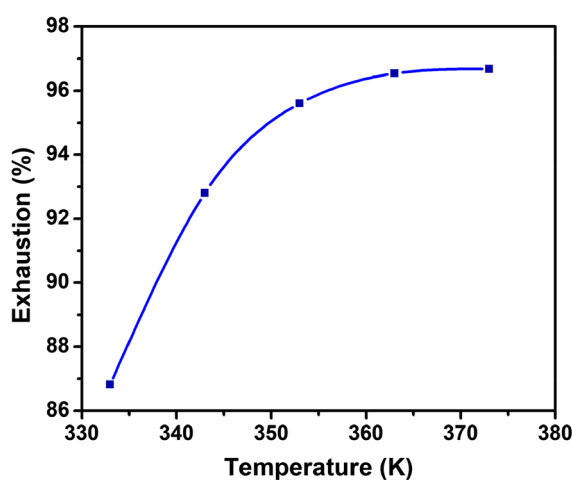


**Fig. 5** Influence of dyeing temperature (333–373 K) on E% with 3% o.w.f of cacao husk extract dye for 90 min dyeing time with a liquor ratio of 20:1

enhanced adsorption capacity of cotton fiber. This specific diffusion mechanism cannot be described by pseudo first-order and pseudo second-order models (Haque et al. 2020). The intraparticle diffusion model was studied to describe the diffusion mechanism of liquid/solid adsorption (Nesic et al. 2012; Weber and Morris 1940). Plots of this model are often multilinear; usually, the data are graphically analyzed to visually determine the straight line segments (Malash and El-Khaiary 2010). In an adsorption process, dye transfer from the dyebath to the fabric can be completed by either film diffusion (transport of dye to fabric surface) or intraparticle diffusion (diffusion of dye within the pores of fabric) or both film diffusion and intraparticle diffusion (Perez-Ameneiro et al. 2015). The intraparticle diffusion mechanism was calculated using Eq. 6 (Hoque et al. 2019; Perez-Ameneiro et al. 2015).

$$[D]_{f,t} = K_{ip}t^{1/2} + C_{ip} \quad (7)$$

where  $K_{ip}$  ( $g \ g^{-1} \ min^{-1/2}$ ) is the intraparticle diffusion rate constant and  $t^{1/2}$  is the square root of time. The constant  $C_{ip}$  ( $g \ g^{-1}$ ) represents the thickness of the boundary layer where a higher value of  $C_{ip}$  indicates a greater influence on the rate control of surface adsorption (Alkan et al. 2007; Li et al. 2012). The graph of  $t^{1/2}$  versus  $[D]_{f,t}$  was plotted, and the slope and intercept were used to derive the appropriate parameters (Fig. 6c). The corresponding model fitting parameters are listed in Table 2 where  $K_{ip1}$ ,  $C_{ip1}$ , and  $R_1^2$  are the slope, intercept, and correlation coefficient of the first linear portion, respectively. Similarly,  $K_{ip2}$ ,  $C_{ip2}$ , and  $R_2^2$  are the slope, intercept and correlation coefficient of the second linear portion, respectively. Likewise,  $K_{ip3}$ ,  $C_{ip3}$ , and  $R_3^2$  specify the slopes, intercepts and correlation coefficients of the third linear portion, respectively. For all temperatures

(333–373 K), plots have multilinear characteristics that consist of three linear sections with different slopes. The first straight line is the external surface diffusion and the sudden increase in slope indicates that the dye molecules are transported to the outer surface of the cotton fabric through film diffusion and the diffusion is rapid at the initial stages with increasing temperature (Tanzifi et al. 2018). As adsorption of the dye molecules starts rapidly on the surface of the cotton fiber and after, the dye molecules gradually start to penetrate inside the cotton fiber through channels (pores) by intraparticle diffusion, and the slope of the second stage is lower than the first stage (Fig. 6c) (Haque et al. 2020). The third part is considered the final equilibrium stage as shown by the lowered diffusion rate (Roy et al. 2013). In this third stage, due to the extremely low concentration of dye in the dyebath, intraparticle diffusion begins to retard (Nesic et al. 2012; Noroozi et al. 2007). In our study, the above statement is also supported by decreasing the diffusion rate of cacao husk extracts dye in progressive steps ( $K_{ip1} > K_{ip2} > K_{ip3}$ ). Besides, the dye transport within the pores of cotton fiber was negatively influenced as the boundary layer thickness increased over time ( $C_{ip3} > C_{ip2} > C_{ip1}$ ). According to the intraparticle diffusion model, it is essential for the  $[D]_{f,t}$  versus  $t^{1/2}$  plots (fitted lines) to pass through the origin (0, 0) if the intraparticle diffusion is considered as the only rate-controlling step over the whole adsorption period (Abraham et al. 2018; Roy et al. 2013). However, the fitted lines (Fig. 6c) do not pass through the origin (i.e. nonzero; 0, 0) and the three-stage adsorption process suggests that both film diffusion and intraparticle diffusion are responsible in controlling the rate of the adsorption process (Li et al. 2012; Nandi et al. 2009). Primarily, at the beginning of the dyeing process, the dye adsorption rate on cotton fabric was controlled by the film diffusion (external mass transport) and at a subsequent stage, the process was controlled by the intraparticle diffusion (Haque et al. 2020).

### Adsorption isotherms

To choose the most appropriate model for the dye adsorption process, the experimental data were evaluated using Langmuir, Freundlich, and Dubinin–Radushkevich adsorption isotherm models. The plot of experimental data is shown in Fig. 7 and the

**Table 1** Substantivity of cacao husk extracts on cotton at different temperatures

Temperature (K)	%E <sub>e</sub>	L	K
333	87.77	20	143.5
343	93.33	20	279.9
353	95.62	20	436.6
363	96.56	20	561.4
373	96.79	20	603.1



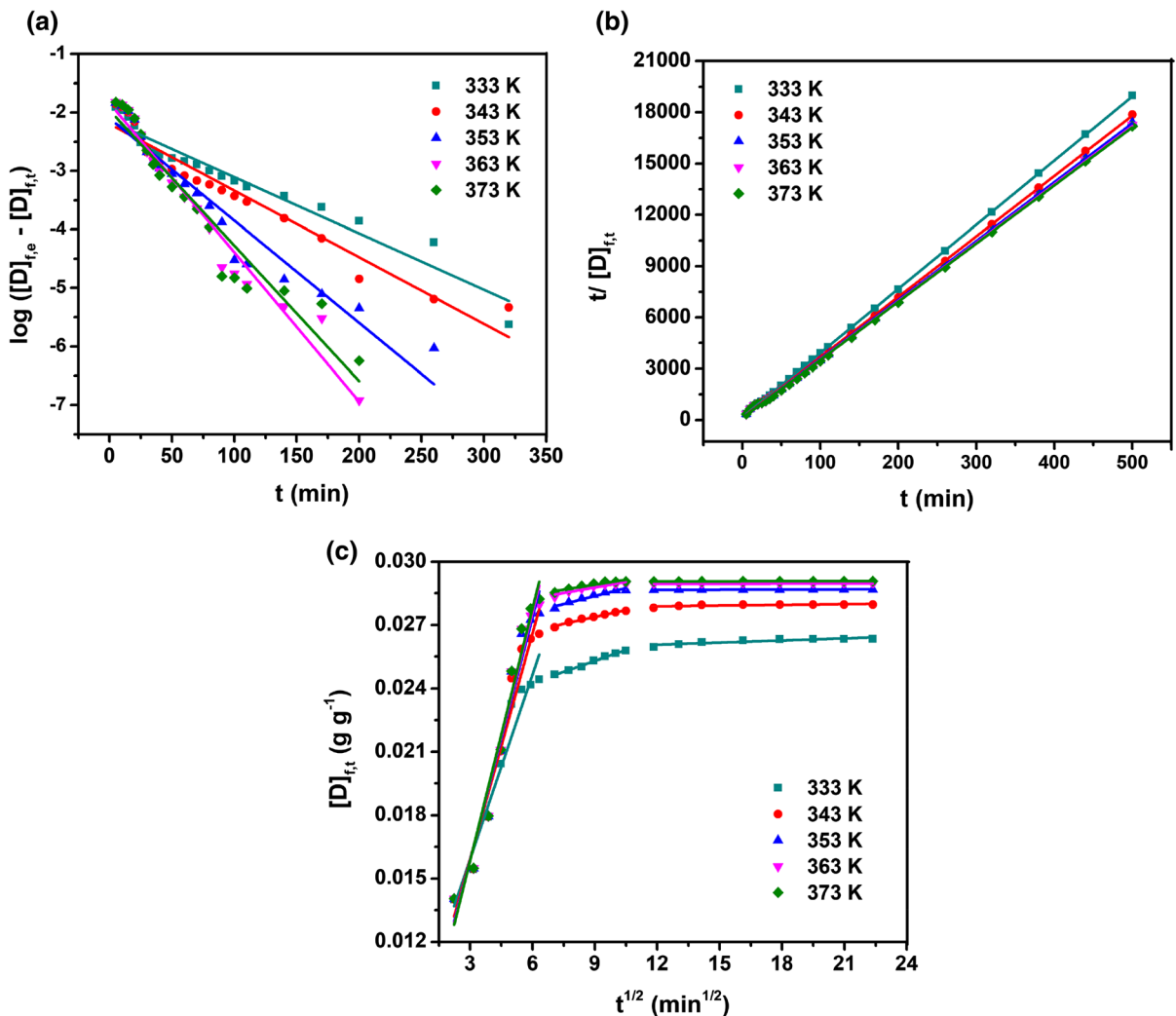


**Fig. 6** Plot of **a** pseudo first-order kinetic model, **b** pseudo second-order kinetic model, and **c** intraparticle diffusion model at different temperatures during the adsorption of cacao husk extracts dye on cotton fabric

corresponding model fitting parameters are presented in Table 3.

The linear form of the Langmuir isotherm model is shown in Eq. 7 (Chanzu et al. 2019; Wang et al. 2018b).

$$\frac{1}{[D]_{f,e}} = \frac{1}{[D]_{\max} \times K_L} \times \frac{1}{[C]_e} + \frac{1}{[D]_{\max}} \quad (8)$$

where  $[D]_{\max}$  ( $\text{g g}^{-1}$ ) is the maximum theoretical saturated adsorption capacity by per unit weight of cotton fabric and it corresponds to a complete monolayer coverage on the surface, and  $K_L$  ( $\text{L g}^{-1}$ ) Langmuir constant, which is related to the energy of adsorption, respectively. The theoretical saturated

adsorption amount,  $[D]_{\max}$ , implies to compare the adsorption performance and indicates the actual limiting adsorption capacity when the surface is entirely covered by adsorbate molecules (Chairat et al. 2005). Correlation coefficients ( $R^2$ ) for different temperatures were more than 0.973, which reflects good fits of this model. The equilibrium parameter ( $r_L$ ), which is also known as the separation factor, was used to study whether the adsorption process was favourable or unfavourable to the Langmuir adsorption model and was derived using Eq. 8 (Cai et al. 2014; Wang et al. 2018b).

**Table 2** Kinetic parameters of pseudo first-order and pseudo second-order kinetic models, and intraparticle diffusion model for cacao husk extract adsorption on cotton fabric at different temperatures

Temp (K)	333	343	353	363	373
$[D]_{f,e}$ (exp) ( $\text{g g}^{-1}$ )	0.0263	0.0280	0.0287	0.0289	0.0290
<i>Pseudo first-order kinetic model</i>					
$K_1$ ( $\text{min}^{-1}$ )	0.0221	0.0262	0.0403	0.0587	0.0534
$[D]_{f,e}$ (cal) ( $\text{g g}^{-1}$ )	0.0072	0.0064	0.0080	0.0144	0.0109
$R_F^2$	0.9418	0.9405	0.9318	0.9677	0.9301
Average: 0.9424					
<i>Pseudo second-order kinetic model</i>					
$K_2$ ( $\text{g g}^{-1} \text{min}^{-1}$ )	8.5186	9.3221	9.8000	9.9742	9.9487
$[D]_{f,e}$ (cal) ( $\text{g g}^{-1}$ )	0.0266	0.0283	0.0290	0.0293	0.0294
$R_S^2$	0.9990	0.9998	0.9997	0.9997	0.9997
Average: 0.9996					
<i>Intraparticle diffusion model</i>					
$K_{ip1}$ ( $\text{g g}^{-1} \text{min}^{-1/2}$ )	$2.91 \times 10^{-3}$	$3.56 \times 10^{-3}$	$3.82 \times 10^{-3}$	$3.91 \times 10^{-3}$	$3.97 \times 10^{-3}$
$C_{ip1}$ ( $\text{g g}^{-1}$ )	$7.81 \times 10^{-3}$	$5.25 \times 10^{-3}$	$4.41 \times 10^{-3}$	$4.14 \times 10^{-3}$	$3.92 \times 10^{-3}$
$R_1^2$	0.9533	0.9579	0.9607	0.9629	0.9653
Average: 0.9600					
$K_{ip2}$ ( $\text{g g}^{-1} \text{min}^{-1/2}$ )	$3.40 \times 10^{-4}$	$2.20 \times 10^{-4}$	$2.50 \times 10^{-4}$	$1.80 \times 10^{-4}$	$1.60 \times 10^{-4}$
$C_{ip2}$ ( $\text{g g}^{-1}$ )	$2.22 \times 10^{-2}$	$2.54 \times 10^{-2}$	$2.61 \times 10^{-2}$	$2.72 \times 10^{-2}$	$2.75 \times 10^{-2}$
$R_2^2$	0.9931	0.9810	0.9546	0.8784	0.9135
Average: 0.9441					
$K_{ip3}$ ( $\text{g g}^{-1} \text{min}^{-1/2}$ )	$3.29 \times 10^{-5}$	$1.11 \times 10^{-5}$	$2.50 \times 10^{-6}$	$1.20 \times 10^{-6}$	$1.70 \times 10^{-6}$
$C_{ip3}$ ( $\text{g g}^{-1}$ )	$2.57 \times 10^{-2}$	$2.77 \times 10^{-2}$	$2.86 \times 10^{-2}$	$2.89 \times 10^{-2}$	$2.90 \times 10^{-2}$
$R_3^2$	0.7927	0.5836	0.9861	0.9403	0.8999
Average: 0.8405					

$$r_L = \frac{1}{1 + K_L[C]_0} \quad (9)$$

where the adsorption isotherm is considered as favourable ( $0 < r_L < 1$ ), unfavourable ( $r_L > 1$ ), linear ( $r_L = 1$ ), and irreversible ( $r_L = 0$ ), respectively, based on the value of  $r_L$  for Langmuir adsorption isotherm model (Cai et al. 2014; Khandaker et al. 2020). The linear form of the Freundlich isotherm model is represented below (Eq. 9) (Abraham et al. 2018; Chanzu et al. 2019).

$$\log[D]_{f,e} = \log K_F + \left(\frac{1}{n}\right) \log[C]_e \quad (10)$$

where  $K_F$  ( $\text{g g}^{-1}$ ) and  $n$  are Freundlich adsorption isotherm constants, which are related to adsorption capacity and intensity of the adsorption, respectively.

The adsorption process is considered as favourable and reflects good adsorption properties when the  $n$  value ranges from 1 to 10 ( $1/n < 1$ ), whereas adsorption is assumed unfavourable if  $1/n > 1$  (Khandaker et al. 2020). A closer value of  $1/n$  to zero correlates to a more heterogeneous adsorbent surface (Hameed et al. 2009; Tanzifi et al. 2018). The average correlation coefficient ( $R^2$ ) of the Langmuir isotherm model was higher than the Freundlich isotherm model. Results indicate that the adsorption process followed the Langmuir adsorption isotherm model and suggests that the adsorption of the cacao husk extracts dye took place on the homogeneous surface of cotton fabric by monolayer adsorption with no interaction between the adjacent adsorbed molecules. The maximum monolayer adsorption capacity  $[D]_{\max}$  was  $0.367 \text{ g g}^{-1}$ . Table 3 shows that all values of separation factor ( $r_L$ )

are in the range  $0 < r_L < 1$ , which suggests that the adsorption process of the cacao husk extracts on the cotton fabric is highly favourable. The value of  $n$  is in the range of 1.02–1.36, which reveals that the adsorption process is favourable and the lower heterogeneous surface is confirmed by the  $1/n$  (0.74–0.98) value (Tanzifi et al. 2018).

The Dubinin–Radushkevich model is a more general model, not based on assumptions of a homogeneous surface or constant adsorption potential, and it can give insight into the biomass porosity and adsorption energy (Inyinbor et al. 2016). Since the mechanism of the adsorption process cannot be determined by the Langmuir and Freundlich adsorption isotherms (Srivastav et al. 2013), for further validation of the adsorption type whether physisorption or chemisorption, the Dubinin–Radushkevich adsorption isotherm model was plotted (Inyinbor et al. 2016). The linear form of the Dubinin–Radushkevich (D-R) isotherm model is shown in Eq. 10 (Haque et al. 2020).

$$\ln[D]_{f,e} = \ln[D]_m - B_{dr}\epsilon^2 \quad (11)$$

where  $\ln [D]_m$  ( $\text{g g}^{-1}$ ) and  $B_{dr}$  ( $\text{mol}^2 \text{J}^{-2}$ ) are the maximum adsorption capacity and D-R adsorption isotherm constant, respectively, and  $\epsilon$  is the constant known as the Polanyi potential, which can be calculated by Eq. 11 (Haque et al. 2020).

$$\epsilon = RT \ln\left(1 + \frac{1}{[C]_e}\right) \quad (12)$$

where  $R$  is the universal gas constant ( $8.314 \text{ J mol}^{-1} \text{ K}^{-1}$ ) and  $T$  is the absolute temperature in Kelvin (K). The D-R adsorption constant ( $B_{dr}$ ) values were used to calculate the mean adsorption energy ( $E$ ) per molecule of the sorbate when it was transferred to the surface of the fabric by using Eq. 12. The value of the mean adsorption energy ( $E$ ) gives information on whether the adsorption process is physical or chemical. When the value of  $E$  is between 8 and  $16 \text{ kJ mol}^{-1}$ , the adsorption process is indicated to be ion-exchange or chemical adsorption, and if the value of  $E$  is below  $8 \text{ kJ mol}^{-1}$ , the adsorption process is said to be physical adsorption in nature (Haque et al. 2020; Srivastav et al. 2013).

$$E = \frac{1}{\sqrt{2B}} \quad (13)$$

A good correlation ( $R^2 > 0.973$ ) of adsorption data with the D-R isotherm model was found and the experimental data fit well with the D-R isotherm. The maximum adsorption capacity  $[D]_m$  obtained by the D-R model is  $0.257 \text{ g g}^{-1}$  and with increasing temperature, the  $[D]_m$  value increased, except at 373 K temperature. In contrast, the values of D-R constants ( $B_{dr}$ ) decreased with increasing temperatures. The mean adsorption energies ( $E$ ) were found to be 3.37, 3.96, 4.39, 4.30, 5.00  $\text{kJ mol}^{-1}$  at 333, 343, 353, 363, and 373 K, respectively. Therefore, the cacao husk extracts dye adsorption onto cotton is a physical adsorption process as the values of  $E$  are less than  $8 \text{ kJ mol}^{-1}$ . This finding is consistent with our previous report (Hossain et al. 2020) with regards to the poor dye fixation rate after the cacao husk extracts/D5 dyeing of cotton fabric. Therefore, it implies that after the cacao husk extracts/D5 dyeing, an auxiliary fixation treatment is essential to improve the dye fixation rate.

## Thermodynamic studies

Thermodynamic studies of an adsorption process are required to understand whether the process is spontaneous, or exothermic or endothermic. To evaluate the thermodynamic feasibility of the adsorption process of cacao husk extract dye onto cotton fabric at different temperatures (333–373 K), basic thermodynamic parameters, including Gibb's free energy change ( $\Delta G^\circ$ ), standard entropy change ( $\Delta S^\circ$ ), and standard enthalpy change ( $\Delta H^\circ$ ) were calculated by using the Van't Hoff equations in Eqs. 13 and 14 (Chairat et al. 2005; Tan et al. 2008).

$$\ln[K]_t = \frac{\Delta S^\circ}{R} - \left(\frac{\Delta H^\circ}{R}\right) \frac{1}{T} \quad (14)$$

$$\Delta G^\circ = \Delta H^\circ - T\Delta S^\circ \quad (15)$$

where  $R$  and the  $T$  are universal gas constant ( $8.314 \text{ J mol}^{-1} \text{ K}$ ) and absolute temperature (K), respectively. In addition,  $[K]_t$  is the distribution coefficient which can be calculated by employing Eq. 15 (Chairat et al. 2005; Tan et al. 2008).

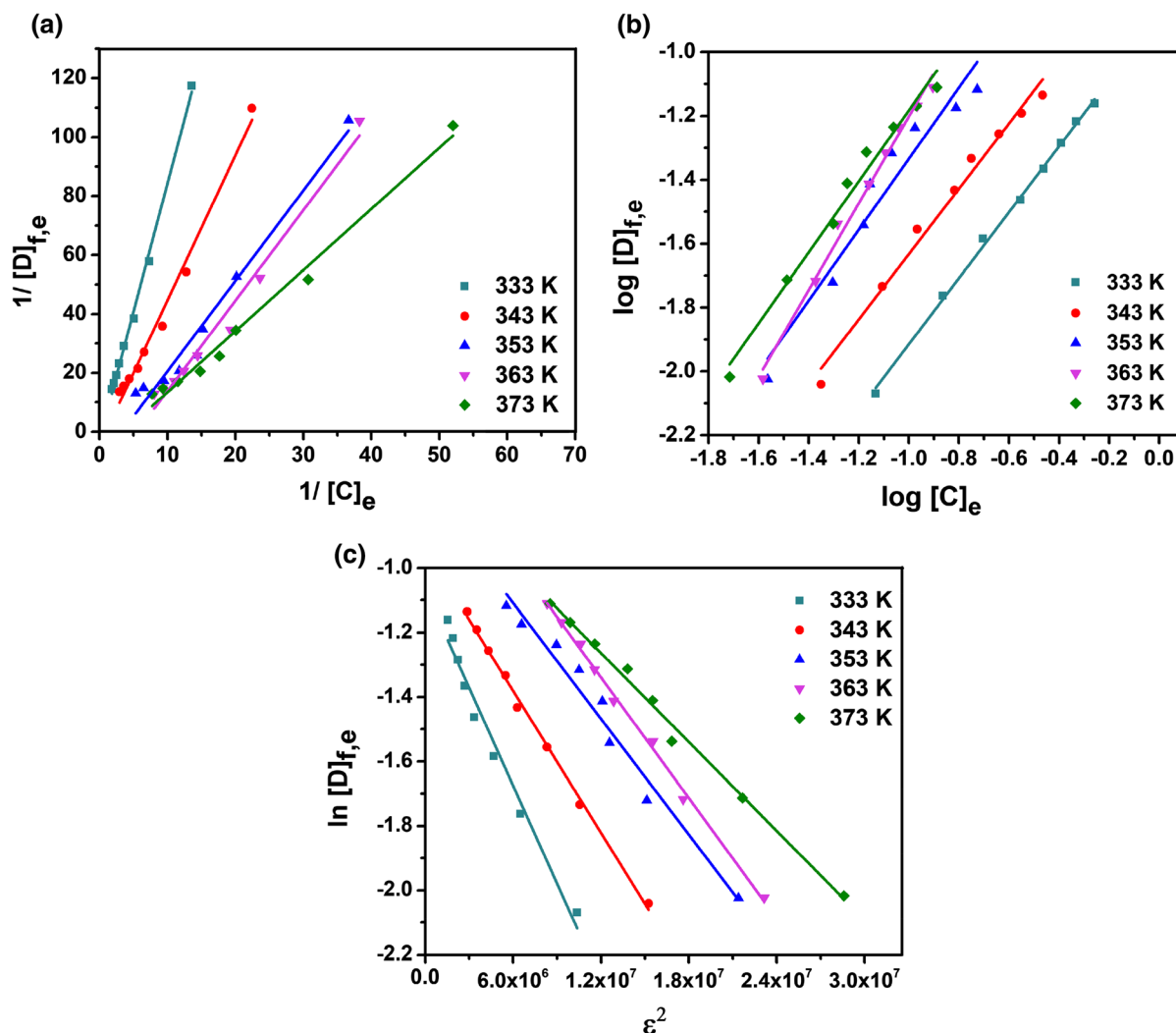


**Fig. 7** Plots of **a** Langmuir, **b** Freundlich, and **c** Dubinin–Radushkevich isotherm models for cacao husk extract dye adsorption on cotton fabric at different temperatures

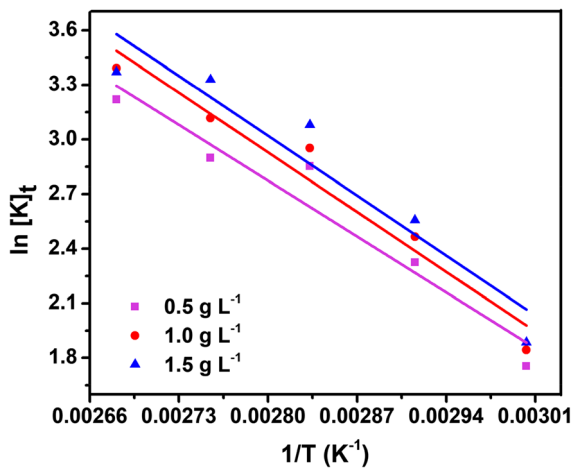
$$[K]_t = \frac{[C]_{a,e}}{[C]_e} \quad (16)$$

where  $[C]_{a,e}$  ( $\text{g L}^{-1}$ ) and  $[C]_e$  ( $\text{g L}^{-1}$ ) are the cacao husk extracts concentration adsorbed and left in the dye bath at equilibrium, respectively. Three different initial dye concentrations ( $C_o = 0.5, 1.0$ , and  $1.5 \text{ g L}^{-1}$ ) were used, and the plots of  $\ln[K]_t$  versus  $1/T$  are shown in Fig. 8. A linear plot with a correlation coefficient  $R^2 > 0.91$  is confirmed in Fig. 8. The thermodynamic parameters  $\Delta H^\circ$  and  $\Delta S^\circ$  were calculated from the slope ( $-\Delta H^\circ/R$ ) and intercept ( $\Delta S^\circ/R$ ) of the Van't Hoff plots (Eq. 13) (Islam et al. 2010). The Gibbs free energy ( $\Delta G^\circ$ ) was calculated by using

the values of  $\Delta H^\circ$  and  $\Delta S^\circ$ , as shown in Eq. 14. The calculated values of  $\Delta G^\circ$ ,  $\Delta H^\circ$ , and  $\Delta S^\circ$  under different dyeing conditions are shown in Table 4 and values of standard enthalpy change ( $\Delta H^\circ$ ) are positive, indicating that the cacao husk extracts dye adsorption was an endothermic process (Inyinbor et al. 2016; Khandaker et al. 2020). The positive values of  $\Delta S^\circ$  specify high affinity of cotton fabric to cacao husk extracts dye and increased randomness at the solid/liquid interface (Inyinbor et al. 2016; Tan et al. 2008). The negative values of  $\Delta G^\circ$  show that the cacao husk extract dye adsorption on cotton fabric was favourable and spontaneous with a high affinity of the adsorbate to the surface of the adsorbent (Inyinbor et al. 2016;

**Table 3** Parameters of Langmuir, Freundlich and Dubinin–Radushkevich adsorption isotherm models for cacao husk extract dye adsorption onto cotton fabric at different temperatures

Temperature (K)	333	343	353	363	373
<i>Langmuir isotherm</i>					
$[D]_{\max}$ (g g <sup>-1</sup> )	0.3666	0.2180	0.0993	0.0595	0.1377
$K_L$ (L g <sup>-1</sup> )	0.3136	0.9312	3.28	5.48	3.51
$r_L$	0.8645	0.6823	0.3786	0.2676	0.3633
$R_L^2$	0.9970	0.9885	0.9735	0.9801	0.9879
Average: 0.9854					
<i>Freundlich isotherm</i>					
N	1.03	1.02	1.11	1.36	1.11
$K_F$ (g g <sup>-1</sup> )	0.1313	0.2454	0.5969	1.4338	0.8482
$R_F^2$	0.9979	0.9857	0.9408	0.9911	0.9834
Average: 0.9797					
<i>Dubinin–Radushkevich isotherm</i>					
$[D]_m$ (g g <sup>-1</sup> )	0.0856	0.1147	0.1781	0.2569	0.1944
$B_{dr}$ (mol <sup>2</sup> kJ <sup>-2</sup> )	$4.40 \times 10^{-8}$	$3.19 \times 10^{-8}$	$2.60 \times 10^{-8}$	$2.71 \times 10^{-8}$	$2.00 \times 10^{-8}$
E (kJ mol <sup>-1</sup> )	3.37	3.96	4.39	4.30	5.00
$R^2$	0.9769	0.9968	0.9726	0.9967	0.9835
Average: 0.9853					

**Fig. 8** Van't Hoff plots,  $\ln [K]_t$  versus  $1/T$  at different initial cacao husk extracts concentrations

Tan et al. 2008). The values of  $\Delta G^\circ$  decreased (higher negative values) with increasing temperature, indicating that the spontaneity of the adsorption process was enhanced with increasing temperature (Inyinbor et al. 2016).

## Conclusions

This research focused on the sustainable waterless dyeing of cotton fabric with natural cacao husk extracts dye using a D5 microemulsion system. The adsorption behavior of cacao husk extracts dye on cotton was studied to understand the dyeing mechanism of natural dye in D5 non-aqueous media, which

**Table 4** Adsorption thermodynamic parameters of cacao husk extract dye onto cotton fabric at different temperatures and initial dye concentrations

Initial concentration (g L <sup>-1</sup> )	$\Delta S^\circ$ (kJ mol <sup>-1</sup> K <sup>-1</sup> )	$\Delta H^\circ$ (kJ mol <sup>-1</sup> )	$\Delta G^\circ$ (kJ mol <sup>-1</sup> )					$R^2$
			333 K	343 K	353 K	363 K	373 K	
0.5	0.125	36.43	- 5.22	- 6.47	- 7.72	- 8.97	- 10.22	0.9391
1.0	0.133	38.95	- 5.48	- 6.81	- 8.15	- 9.48	- 10.81	0.9564
1.5	0.135	39.05	- 5.72	- 7.07	- 8.41	- 9.76	- 11.10	0.9119



improved the dyeing performance. The research results demonstrate that a higher dye uptake was achieved using a D5 microemulsion system and almost 97% of the cacao husk extracts was adsorbed into the cotton fiber. The pseudo second-order kinetic model fit well with the adsorption process. The adsorption equilibrium isotherm was best fitted to the Langmuir isotherm model. The Dubinin–Radushkevich adsorption isotherm model specified that the cacao husk extracts dyeing of cotton fabric was a physical adsorption process. The positive value of  $\Delta S^\circ$  signified that the randomness of the solid-liquid interface increased during cacao husk extracts adsorption on cotton fabric in D5 microemulsion. The negative values of  $\Delta G^\circ$  indicated the spontaneous nature of adsorption, while the positive values of  $\Delta H^\circ$  showed that the adsorption reaction was endothermic. Therefore, non-aqueous dyeing technology provides an innovative way to achieve a higher absorption rate of natural dyes. This research suggests a low residual effluent-free dyeing of cotton fabric due to excellent dyebath exhaustion by using the cacao husk extract dye/D5 microemulsion system, which is a clean dyeing process that saves water and environment. The developed process could be utilized in the industry level for the sustainable dyeing of textiles.

**Author contributions** Conceptualization: YC, XY; Methodology: Md.YH, WZ, Md.NP; Formal analysis and investigation: Md.YH, WZ, Md.NP; Writing - original draft preparation: Md.YH, WZ, Md.NP, SS; Writing - review and editing: MMH, Md.IUIH, VN; Funding acquisition: YC, XY; Supervision: YC, XY.

**Funding** This work was financially supported by the China National Textile & Apparel Council (2013“Textile Vision” Applied Basic Research, 2013 – 153), and Hubei Province Science and Technology Support Program (Grant No. 2013BAA043).

**Availability of data and material** The datasets generated during the current study are available from the corresponding author on reasonable request (Prof. Yingjie Cai).

**Code availability** No code was attempted or used during the current manuscript.

**Compliance with ethical standards**

**Conflict of interest** The authors have no conflicts of interest to declare that are relevant to the content of this article.

**Ethical approval** This manuscript does not contain any studies with human participants or animals performed by any of the authors.

## References

- Abraham R, Mathew S, Kurian S, Saravanakumar M, Ealias AM, George G (2018) Facile synthesis, growth process, characterisation of a nanourchin-structured  $\alpha$ -MnO<sub>2</sub> and their application on ultrasonic-assisted adsorptive removal of cationic dyes: A half-life and half-capacity concentration approach. *Ultrason Sonochem* 49:175–189. <https://doi.org/10.1016/j.ultsonch.2018.07.045>
- Abraham R, Mathew S, Kurian S, Saravanakumar M, Ealias AM, George G (2018) Facile synthesis, growth process, characterisation of a nanourchin-structured  $\alpha$ -MnO<sub>2</sub> and their application on ultrasonic-assisted adsorptive removal of cationic dyes: a half-life and half-capacity concentration approach. *Ultrason Sonochem* 49:175–189. <https://doi.org/10.1016/j.ultsonch.2018.07.045>
- Alkan M, Demirbaş Ö, Doğan M (2007) Adsorption kinetics and thermodynamics of an anionic dye onto sepiolite. *Micropor Mesopor Mat* 101:388–396. <https://doi.org/10.1016/j.micromeso.2006.12.007>
- Cai Y, Huang Y, Liu F, He L, Lin L, Zeng Q (2014) Liquid ammonia dyeing of cationic ramie yarn with tri-azinylnbsp;reactive dyes. *Cellulose* 21:3841–3849. <https://doi.org/10.1007/s10570-014-0393-1>
- Cai Y, Liang Y, Navik R, Zhu W, Zhang C, Pervez MN, Wang Q (2020) Improved reactive dye fixation on ramie fiber in liquid ammonia and optimization of fixation parameters using the Taguchi&nbsp;approach. *Dyes Pigments* 183:108734. <https://doi.org/10.1016/j.dyepig.2020.108734>
- Cai Y, Su S, Navik R, Wen S, Peng X, Pervez MN, Lin L (2018) Cationic modification of ramie fibers in&nbsp;liquid ammonia. *Cellulose* 25:4463–4475. <https://doi.org/10.1007/s10570-018-1905-1>
- Chairat M, Rattanaphani S, Bremner JB, Rattanaphani V (2005) An adsorption and kinetic study of lac dyeing on silk. *Dyes Pigments* 64:231–241. <https://doi.org/10.1016/j.dyepig.2004.06.009>
- Chanzu HA, Onyari JM, Shiundu PM (2019) Brewers’ spent grain in adsorption of aqueous Congo Red and malachite Green dyes: Batch and continuous flow systems. *J Hazard Mater* 380:120897. <https://doi.org/10.1016/j.jhazmat.2019.120897>
- Chen L, Wang B, Ruan X, Chen J, Yang Y (2015) Hydrolysis-free and fully recyclable reactive dyeing of cotton in green, non-nucleophilic solvents for a sustainable textile industry. *J Clean Prod* 107:550–556. <https://doi.org/10.1016/j.jclepro.2015.05.144>
- Ferus-Comelo M (2013) An analysis of the substantivity of hydrolysed reactive dyes and its implication for rinsing processes. *Color Technol* 129:24–31. <https://doi.org/10.1111/j.1478-4408.2012.00405.x>
- Gorjanc M, Savić A, Topalić-Trivunović L, Mozetić M, Vesel A, Grujić D (2016) Dyeing of plasma treated cotton and bamboo rayon with *Fallopia japonica* extract. *Cellulose*

- 23:2221–2228. <https://doi.org/10.1007/s10570-016-0951-9>
- Halysh V, Sevastyanova O, Riazanova AV, Pasalskiy B, Budnyak T, Lindström ME, Kartel M (2018) Walnut shells as a potential low-cost lignocellulosic sorbent for dyes and metal ions. *Cellulose* 25:4729–4742. <https://doi.org/10.1007/s10570-018-1896-y>
- Hameed BH, Salman JM, Ahmad AL (2009) Adsorption isotherm and kinetic modeling of 2,4-D pesticide on activated carbon derived from date stones. *J Hazard Mater* 163:121–126. <https://doi.org/10.1016/j.jhazmat.2008.06.069>
- Haque ANM, Remadevi R, Rojas OJ, Wang X, Naebe M (2020) Kinetics and equilibrium adsorption of methylene blue onto cotton gin and trash bioadsorbents. *Cellulose* 27:6485–6504. <https://doi.org/10.1007/s10570-020-03238-y>
- Hong KH, Bae JH, Jin SR, Yang JS (2012) Preparation and properties of multi-functionalized cotton fabrics treated by extracts of gromwell and gallnut. *Cellulose* 19:507–515. <https://doi.org/10.1007/s10570-011-9613-0>
- Hoque MIU et al (2019) A facile synthesis of hematite nanorods from rice starch and their application to Pb (II) ions removal. *ChemistrySelect* 4:3730–3736. <https://doi.org/10.1002/slct.201802462>
- Hossain MY, Liang Y, Pervez MN, Ye X, Dong X, Hassan MM, Cai Y (2020) Effluent-free deep dyeing of cotton fabric with cacao husk extracts using the Taguchi optimization method. *Cellulose*. <https://doi.org/10.1007/s10570-020-03525-8>
- Inyinbor A, Adekola F, Olatunji GA (2016) Kinetics, isotherms and thermodynamic modeling of liquid phase adsorption of Rhodamine B dye onto Raphia hookerie fruit epicarp. *Water Resour Ind* 15:14–27. <https://doi.org/10.1016/j.wri.2016.06.001>
- Islam MA, Ali I, Karim SA, Firoz MSH, Chowdhury A-N, Morton DW, Angove MJ (2019) Removal of dye from polluted water using novel nano manganese oxide-based materials. *J Water Process Eng* 32:100911. <https://doi.org/10.1016/j.jwpe.2019.100911>
- Islam M, Mishra PC, Patel R (2010) Physicochemical characterization of hydroxyapatite and its application towards removal of nitrate from water. *J Environ Manage* 91:1883–1891. <https://doi.org/10.1016/j.jenvman.2010.04.013>
- Islam MA, Morton DW, Johnson BB, Mainali B, Angove MJ (2018) Manganese oxides and their application to metal ion and contaminant removal from wastewater. *J Water Process Eng* 26:264–280. <https://doi.org/10.1016/j.jwpe.2018.10.018>
- İşmal ÖE, Yıldırım L (2019) 3 - Metal mordants and biomordants. In: Shahid ul I, Butola BS (eds) *The Impact and Prospects of Green Chemistry for Textile Technology*. Woodhead Publishing, Cambridge, pp 57–82. <https://doi.org/10.1016/B978-0-08-102491-1.00003-4>
- Khandaker S, Toyohara Y, Saha GC, Awual MR, Kuba T (2020) Development of synthetic zeolites from bio-slag for cesium adsorption: kinetic, isotherm and thermodynamic studies. *J Water Process Eng* 33:101055. <https://doi.org/10.1016/j.jwpe.2019.101055>
- Li Y et al (2012) Equilibrium, kinetic and thermodynamic studies on the adsorption of phenol onto graphene. *Mater Res Bull* 47:1898–1904. <https://doi.org/10.1016/j.materresbull.2012.04.021>
- Liman MLR, Islam MT, Hossain MM, Sarker P, Dabnath S (2020) Coloration of cotton fabric using watermelon extract: mechanism of dye-fiber bonding and chromophore absorption. *J Text Inst.* <https://doi.org/10.1080/00405000.2020.1738036>
- Malash GF, El-Khaiary MI (2010) Piecewise linear regression: a statistical method for the analysis of experimental adsorption data by the intraparticle-diffusion models. *Chem Eng J* 163:256–263. <https://doi.org/10.1016/j.cej.2010.07.059>
- Morshed MN, Pervez MN, Behary N, Bouazizi N, Guan J, Nierstrasz VA (2020) Statistical modeling and optimization of heterogeneous Fenton-like removal of organic pollutant using fibrous catalysts: a full factorial design. *Sci Rep* 10:1–14. <https://doi.org/10.1038/s41598-020-72401-z>
- Moussout H, Ahlafi H, Aazza M, Maghat H (2018) Critical of linear and nonlinear equations of pseudo-first order and pseudo-second order kinetic models. *Int J Mod Sci* 4:244–254. <https://doi.org/10.1016/j.kijoms.2018.04.001>
- Nandi BK, Goswami A, Purkait MK (2009) Adsorption characteristics of brilliant green dye on kaolin. *J Hazard Mater* 161:387–395. <https://doi.org/10.1016/j.jhazmat.2008.03.110>
- Nesic AR, Velickovic SJ, Antonovic DG (2012) Characterization of chitosan/montmorillonite membranes as adsorbents for Bezactiv Orange V-3R dye. *J Hazard Mater* 209:256–263. <https://doi.org/10.1016/j.jhazmat.2012.01.020>
- Noroozi B, Sorial G, Bahrani H, Arami M (2007) Equilibrium and kinetic adsorption study of a cationic dye by a natural adsorbent—Silkworm and pupa. *J Hazard Mater* 139:167–174. <https://doi.org/10.1016/j.jhazmat.2006.06.021>
- Pei L, Luo Y, Gu X, Dou H, Wang J (2019) Diffusion mechanism of aqueous solutions and swelling of cellulosic fibers in silicone non-aqueous dyeing system. *Polymers* 11:411. <https://doi.org/10.3390/polym11030411>
- Perez-Ameneiro M, Vecino X, Cruz J, Moldes A (2015) Wastewater treatment enhancement by applying a lipopeptide biosurfactant to a lignocellulosic biocomposite. *Carbohydr Polym* 131:186–196. <https://doi.org/10.1016/j.carbpol.2015.05.075>
- Pervez M, He W, Zarra T, Naddeo V, Zhao Y (2020) New sustainable approach for the production of Fe<sub>3</sub>O<sub>4</sub>/graphene oxide-activated persulfate system for dye removal in real wastewater. *Water* 12:733. <https://doi.org/10.3390/w12030733>
- Pervez MN, Stylios GK, Liang Y, Ouyang F, Cai Y (2020) Low-temperature synthesis of novel polyvinylalcohol (PVA) nanofibrous membranes for catalytic dye degradation. *J Clean Prod.* <https://doi.org/10.1016/j.jclepro.2020.121301>
- Rehman A et al (2018) Simultaneous dyeing and anti-bacterial finishing on 100% cotton fabric: process establishment and characterization. *Cellulose* 25:5405–5414. <https://doi.org/10.1007/s10570-018-1934-9>

- Risner CH (2008) Simultaneous determination of theobromine, (+)-catechin, caffeine, and (–)-epicatechin in standard reference material baking chocolate 2384, cocoa, cocoa beans, and cocoa butter. *J Chromatogr Sci* 46:892–899. <https://doi.org/10.1093/chromsci/46.10.892>
- Roy A, Adhikari B, Majumder S (2013) Equilibrium, kinetic, and thermodynamic studies of azo dye adsorption from aqueous solution by chemically modified lignocellulosic jute fiber. *Ind Eng Chem Res* 52:6502–6512. <https://doi.org/10.1021/ie400236s>
- Salager J-L, Forgiarini AM, Márquez L, Manchego L, Bullón J (2013) How to attain an ultralow interfacial tension and a three-phase behavior with a surfactant formulation for enhanced oil recovery: a review. Part 2. Performance improvement trends from Winsor's premise to currently proposed inter- and intra-molecular mixtures. *J Surfactants Deterg* 16:631–663. <https://doi.org/10.1007/s11743-013-1485-x>
- Samanta AK, Konar A (2011) Dyeing of textiles with natural dyes. *Natural dyes*. InTech, Rijeka. <https://doi.org/10.5772/21341>
- Simonin J-P (2016) On the comparison of pseudo-first order and pseudo-second order rate laws in the modeling of adsorption kinetics. *Chem Eng J* 300:254–263. <https://doi.org/10.1016/j.cej.2016.04.079>
- Srivastav AL, Singh PK, Srivastava V, Sharma YC (2013) Application of a new adsorbent for fluoride removal from aqueous solutions. *J Hazard Mater* 263:342–352. <https://doi.org/10.1016/j.jhazmat.2013.04.017>
- Su S et al (2019) Anhydrous dyeing processes of ramie fiber in liquid ammonia. *Cellulose* 26:8109–8120. <https://doi.org/10.1007/s10570-019-02630-7>
- Tan I, Ahmad A, Hameed B (2008) Adsorption of basic dye on high-surface-area activated carbon prepared from coconut husk: equilibrium, kinetic and thermodynamic studies. *J Hazard Mater* 154:337–346. <https://doi.org/10.1016/j.jhazmat.2007.10.031>
- Tang S et al (2019) Dye adsorption by self-recoverable, adjustable amphiphilic graphene aerogel. *J Colloid Interf Sci* 554:682–691. <https://doi.org/10.1016/j.jcis.2019.07.041>
- Tang AY, Kan C (2020) Non-aqueous dyeing of cotton fibre with reactive dyes: a review. *Color Technol*. <https://doi.org/10.1111/cote.12459>
- Tang AY, Wang YM, Lee CH, Kan C-W (2017) Computer color matching and levelness of PEG-based reverse micellar decamethyl cyclopentasiloxane (D5) solvent-assisted reactive dyeing on cotton fiber. *Appl Sci* 7:682. <https://doi.org/10.3390/app7070682>
- Tanzifi M et al. (2018) Adsorption of Amido Black 10B from aqueous solution using polyaniline/SiO<sub>2</sub>nanocomposite: Experimental investigation and artificial neural network modeling. *J Colloid Interf Sci* 510:246–261. <https://doi.org/10.1016/j.jcis.2017.09.055>
- Tsatsaroni E, Liakopoulou-Kyriakides M (1995) Effect of enzymatic treatment on the dyeing of cotton and wool fibres with natural dyes. *Dyes Pigments* 29:203–209. [https://doi.org/10.1016/0143-7208\(95\)00044-G](https://doi.org/10.1016/0143-7208(95)00044-G)
- Wang J, Gao Y, Zhu L, Gu X, Dou H, Pei L (2018) Dyeing property and adsorption kinetics of reactive dyes for cotton textiles in salt-free non-aqueous. *Dyeing Syst Polym* 10:1030. <https://doi.org/10.3390/polym10091030>
- Wang X, Jiang C, Hou B, Wang Y, Hao C, Wu J (2018) Carbon composite lignin-based adsorbents for the adsorption of dyes. *Chemosphere* 206:587–596. <https://doi.org/10.1016/j.chemosphere.2018.04.183>
- Wang Y, Lee C-h, Tang Y-l, Kan C-w (2016) Dyeing cotton in alkane solvent using polyethylene glycol-based reverse micelle as reactive dye carrier. *Cellulose* 23:965–980. <https://doi.org/10.1007/s10570-015-0831-8>
- Weber WJ, Morris JC (1940) Kinetics of adsorption on carbon from solution. *J San Eng Div* 89:31–60

**Publisher's note** Springer Nature remains neutral with regard to jurisdictional claims in published maps and institutional affiliations.